Microbiology (2006), **152**, 591–604 DOI 10.1099/mic.0.28571-0

Calcineurin, Mpk1 and Hog1 MAPK pathways independently control fludioxonil antifungal sensitivity in *Cryptococcus neoformans*

Kaihei Kojima,[1] Yong-Sun Bahn[1] and Joseph Heitman[1,2,3,4]

Departments of Molecular Genetics and Microbiology[1], Pharmacology and Cancer Biology[2] and Medicine[3], and Duke University Medical Center[4], Durham, NC 27710, USA

Correspondence
Joseph Heitman
heitm001@duke.edu

Received 6 October 2005
Revised 1 December 2005
Accepted 3 December 2005

Fludioxonil is employed as an agricultural fungicide to control plant-pathogenic fungi such as *Botrytis cinerea*. *Cryptococcus neoformans* is a basidiomycetous human fungal pathogen that causes fatal disease in immunocompromised hosts. This paper demonstrates that three different signalling cascades regulate sensitivity of *C. neoformans* to fludioxonil. Fludioxonil inhibited growth of the serotype A sequence reference strain H99 but not that of the sequenced serotype D strain JEC21. In the drug-sensitive wild-type strain, fludioxonil exposure activated the Hog1 osmosensing pathway, and *hog1*Δ mutations conferred fludioxonil resistance. Fludioxonil treatment caused cell growth inhibition following cell swelling and cytokinesis defects in the sensitive wild-type but not in a *hog1*Δ mutant strain, suggesting that Hog1 activation results in morphological cellular defects. Fludioxonil exerted a fungistatic effect on the wild-type strain H99, but exhibited fungicidal activity against calcineurin mutant strains, indicating that the calcineurin pathway contributes to drug resistance in this fungus. Combination of fludioxonil and the calcineurin inhibitor FK506 synergistically inhibited *C. neoformans* growth. *mpk1*Δ MAPK mutant strains exhibited fludioxonil hypersensitivity, indicating that this pathway also contributes to drug resistance. These studies provide evidence that the broad-spectrum antifungal drug fludioxonil exerts its action via activation of the Hog1 MAPK pathway and provide insight into novel targets for synergistic antifungal drug combinations.

INTRODUCTION

The basidiomycetous fungus *Cryptococcus neoformans* is an opportunistic pathogen that infects the central nervous system of immunocompromised patients, causing life-threatening meningoencephalitis (Hull & Heitman, 2002). Cryptococcosis is one of the most common fungal infections diagnosed in AIDS patients, particularly in regions where antifungal drugs such as amphotericin B and fluconazole are not readily available. However, amphotericin B has a number of adverse side effects and fluconazole exhibits only fungistatic activity. Furthermore, mutants resistant to these drugs are emerging in *Candida* species and *Cryptococcus neoformans* (Cameron *et al.*, 1993; Paugam *et al.*, 1994; White *et al.*, 1998). Therefore, it has become an important issue to develop new antifungal agents that are fungicidal, less toxic, and employ different mechanisms of action for use in combination drug therapies.

Abbreviations: 5-FOA, 5-fluoroorotic acid; dH_2O, distilled water; FIC, fractional inhibitory concentration; MFC, minimal fungicidal concentration; WT, wild-type.

A table of primer sequences is available with the online version of this paper.

Fludioxonil [4-(2,2-difluoro-1,3-benzodioxol-4-yl)pyrrole-3-carbonitrile] is a phenylpyrrole antifungal drug derived from the antibiotic pyrrolnitrin (Gehmann *et al.*, 1990); it has a broad antifungal spectrum and is now used to control a variety of important plant-pathogenic fungi. It is a unique antifungal drug that targets signal transduction. Several lines of evidence implicate the Hog1 MAP kinase (MAPK) pathway in fludioxonil-mediated antifungal effects. In the filamentous fungus *Neurospora crassa*, the *OS-2* gene, a homologue of the *Saccharomyces cerevisiae HOG1* gene, is responsible for adapting to hyperosmotic conditions by accumulating intracellular glycerol, and its deletion causes hyperosmosensitivity and resistance to fludioxonil (Zhang *et al.*, 2002). Exposure of several plant-pathogenic fungi to fludioxonil, including *Colletotrichum lagenarium*, *Botrytis cinerea* and *Cochliobolus heterostrophus*, activates the Hog1 MAPK homologue and inhibits fungal growth (Kojima *et al.*, 2004). In *Candida albicans* and *N. crassa*, fludioxonil treatment seems to induce excessive intracellular glycerol accumulation (Fujimura *et al.*, 2000a; Ochiai *et al.*, 2002; Zhang *et al.*, 2002).

Tacrolimus (FK506) and cyclosporin A (CsA) were both originally isolated as immunosuppressive agents (Borel, 1976; Kino *et al.*, 1987) and also exhibit potential antifungal activity (Odom *et al.*, 1997a; Perfect & Durack, 1985). These

drugs exert their toxic effect by binding to target immunophilins and subsequently inhibiting calcineurin activity (Cruz *et al.*, 2000; Odom *et al.*, 1997a). In *Cryptococcus neoformans*, inhibition of calcineurin by FK506 causes a growth defect at high temperature. Similar to drug inhibition, mutation of the calcineurin A (*CNA1*) or calcineurin B (*CNB1*) genes renders cells inviable at high temperature (Fox *et al.*, 2001; Odom *et al.*, 1997b) and severely attenuates virulence of *C. neoformans*. Furthermore, the calcineurin pathway is involved in mating and cell wall integrity of *C. neoformans* (Cruz *et al.*, 2001; Kraus *et al.*, 2003).

Combination treatment with multiple drugs can exert a more potent antifungal activity than treatment with a single drug. For instance, FK506 exhibits synergistic antifungal action against *C. neoformans* with several other drugs in both calcineurin-dependent and -independent manners. Inhibition of calcineurin by FK506 is required for its synergy with the echinocandins, but is not required for FK506-mediated synergy with fluconazole (Del Poeta *et al.*, 2000), indicating another effect of FK506 on cells in addition to calcineurin inhibition. Similarly, the toxic action of fludioxonil may be exerted via other signal transduction pathways in addition to the Hog1 MAPK pathway. In *N. crassa*, a cAMP- and calcium-independent protein kinase is inhibited by phenylpyrroles, including fludioxonil (Pillonel & Mayer, 1997). On the other hand, in *Ustilago maydis*, mutants lacking cAMP-dependent protein kinase A (PKA) exhibit increased resistance to dicarboximide fungicides, although these fungicides do not directly inhibit PKA (Orth *et al.*, 1995; Ramesh *et al.*, 2001). Interestingly, a *Colletotrichum lagenarium* mutant lacking the PKA regulatory subunit shows significantly increased sensitivity to fludioxonil (Kojima *et al.*, 2004). These results indicate that these signalling pathways could also be useful targets for designing novel antifungal agents. Therefore, elucidating the relationships between drugs and their target signal transduction pathways may provide the foundation for new combination drug therapies and less toxic therapies.

In this study, we demonstrate that the Hog1 MAPK pathway promotes sensitivity to fludioxonil in *C. neoformans*, whereas the calcineurin and Mpk1 MAPK pathways mediate resistance to fludioxonil. Furthermore, we provide evidence that simultaneous perturbation of the Hog1 and calcineurin pathways by combined treatment with fludioxonil and FK506 inhibits the growth of the pathogen even more effectively. Biochemical and genetic data demonstrate that fludioxonil exerts its cytotoxic effects through hyperactivation of the Hog1 pathway and that cell wall integrity plays an important role in maintaining cell viability in the presence of fludioxonil.

METHODS

Strains and culture conditions. Strains used in this study are listed in Table 1. Among clinical serotype A strains, IN-38 is from

Table 1. Strains used in this study

Each NAT-STM# indicates a Nat^r marker with a unique signature tag. Information about clinical and environmental strains described in Fig. 4 is available on request.

Strain	Serotype	Genotype	Reference
H99	A	*MATα*	Perfect *et al.* (1993)
H99	A	*MATα ura5*	Lengeler *et al.* (2001)
JEC171	D	*MAT***a** *lys2 ade2*	Moore & Edman (1993)
JEC21	D	*MATα*	Kwon-Chung *et al.* (1992)
KBL-AD1	AD	*MAT***a**/*α URA5*/*ura5 LYS2*/*lys2 ADE2*/*ade2*	Lengeler *et al.* (2001)
KBL-AD2	AD	*MAT***a**/*α URA5*/*ura5 LYS2*/*lys2 ADE2*/*ade2*	Lengeler *et al.* (2001)
KBL-AD3	AD	*MAT***a**/*α URA5*/*ura5 LYS2*/*lys2 ADE2*/*ade2*	Lengeler *et al.* (2001)
KBL-AD4	AD	*MAT***a**/*α URA5*/*ura5 LYS2*/*lys2 ADE2*/*ade2*	Lengeler *et al.* (2001)
KK1	A	*MATα cna1*Δ::*NAT-STM#117*	This study
KK2	A	*MATα cnb1*Δ::*NAT-STM#122*	This study
KK3	A	*MATα mpk1*Δ::*NAT-STM#150*	This study
KK4	A	*MATα cna1*Δ::*NEO hog1*Δ::*NAT#177*	This study
KK5	A	*MATα cna1*Δ::*NAT-STM#117 CNA1*::*NEO*	This study
YSB64	A	*MATα hog1*Δ::*NAT-STM#177*	Bahn *et al.* (2005)
YSB123	A	*MATα pbs2*Δ::*NAT-STM#213*	Bahn *et al.* (2005)
YSB139	D	*MATα hog1*Δ::*NAT-STM#177*	Bahn *et al.* (2005)
YSB145	A	*MATα hog1*Δ::*NAT-STM#177 HOG1-NEO*	Bahn *et al.* (2005)
YSB212	A	*MATα pbs2*Δ::*NAT-STM#213 PBS2*::*NEO*	Bahn *et al.* (2005)
YSB253	A	*MATα hog1*Δ::*NAT-STM#177 HOG1*$^{T171A+Y173A}$*-NEO*	Bahn *et al.* (2005)
YSB273	A	*MATα bck1*Δ::*NAT-STM#43*	This study
YSB308	A	*MATα hog1*Δ::*NAT-STM#177 HOG1*$^{K49S+K50N}$*-NEO*	Bahn *et al.* (2005)
YSB330	A	*MATα mkk1*Δ::*NAT-STM#224*	This study

India; UG-20020 is from Uganda. Other serotype A and D clinical or environmental strains were described previously (Bahn *et al.*, 2005). AD hybrid strains were previously generated by crossing the serotype D strain JEC171 (*MAT***a** *ade2 lys2*) and a 5-fluoroorotic acid (5-FOA)-resistant mutant of the serotype A strain H99 (*MAT*α *ura5*) (Lengeler *et al.*, 2001). The *S. cerevisiae hog1*/*hog1* mutant (from the diploid homozygous deletion mutant collection) and its parental strain BY4743 (diploid of strains BY4741/BY4742; Giaever *et al.*, 2002) were also used. YPD medium contained 2 % (v/v) glucose, 2 % (w/v) Bacto Peptone (Difco), and 1 % (w/v) yeast extract (Difco). YPD agar plates also contained 2 % (w/v) Bacto Agar (Difco). The top agar used in these assays was 0·7 % Bacto Agar (Difco) in water.

Disk diffusion halo assays. Strains were inoculated into liquid YPD medium and grown overnight at 30 °C. The cells were washed three times with sterile distilled water (dH_2O), and counted with a haemocytometer. Approximately 2×10^7 cells were inoculated into 8 ml top agar prewarmed at 42 °C then spread onto 150 mm diameter YPD plates, and allowed to dry. Fludioxonil (Sigma) was dissolved in dimethyl sulfoxide; FK506 (Fujisawa) was dissolved in 90 % ethanol and 10 % Tween 20. Drugs and the solvent controls were applied to sterile 6-mm-diameter BBL disks (Becton Dickinson). These disks were then placed on the solidified top agar surface as indicated, and the strains were grown at 30 °C for 48 h.

Disruption of the *CNA1*, *CNB1*, *MPK1*, *MKK1* and *BCK1* genes. The *CNA1*, *CNB1*, *MPK1*, *MKK1* and *BCK1* genes were disrupted by biolistic transformation in *C. neoformans* serotype A strain H99 with alleles generated by PCR overlap as previously described (Davidson *et al.*, 2002). The 5′ and 3′ regions of these genes were PCR-amplified with the following primers: 12339/12409 and 12408/12336 for the 5′ and 3′ regions of the *CNA1* gene respectively, 12347/12412 and 12410/12344 for the *CNB1* gene, 13460/13461 and 13462/13463 for the *MPK1* gene, 14419/14420 and 14421/14422 for the *MKK1* gene, and 13979/13980 and 13981/13982 for the *BCK1* gene (see supplementary Table S1, available with the online version of this paper, for the primer sequences). M13 forward (M13F) and reverse (M13R) primers were used to generate the Nat^r (nourseothricin acetyltransferase) dominant selectable marker with plasmids pNATSTM with a unique sequence tag (#117 for the *CNA1* gene, #122 for the *CNB1* gene, #150 for the *MPK1* gene, #224 for the *MKK1* gene, #43 for the *BCK1* gene, kindly provided by Dr Jennifer K. Lodge, Saint Louis University School of Medicine; tag sequence is available upon request) as templates (Hensel *et al.*, 1995). The disruption alleles of these genes were generated by PCR overlap using primers 12339/12336 for the *CNA1* gene, 12347/12344 for the *CNB1* gene, 13460/13463 for the *MPK1* gene, 14419/14422 for the *MKK1* gene, and 13979/13982 for the *BCK1* gene.

The gel-extracted disruption cassettes were precipitated onto 600 μg of gold microcarrier beads (0·8 μm, bioWORLD) and biolistically transformed into the serotype A strain H99. Stable transformants were selected on YPD medium containing nourseothricin (100 mg l^{-1}). The *cna1*Δ, *cnb1*Δ, *mpk1*Δ, *mkk1*Δ and *bck1*Δ mutant strains were screened by diagnostic PCR for the 5′ and 3′ junctions and by Southern blot analysis using specific probes generated by PCR with primers 12343/12342 for the *CNA1* gene, 12351/12350 for the *CNB1* gene, 13466/13467 for the *MPK1* gene, 14424/14425 for the *MKK1* gene and 13979/13980 for the *BCK1* gene.

To construct the serotype A *cna1*Δ *hog1*Δ strain, M13F and M13R primers were used to generate the Neo^r (neomycin phosphotransferase II) dominant selectable markers with template pJAF1 (Fraser *et al.*, 2003). The *cna1*Δ::*NEO* disruption allele was generated by PCR overlap with primers 12339/12336 and biolistically transformed into the *hog1*Δ mutant strain (YSB64). Stable transformants were selected on YPD agar containing both nourseothricin (100 mg l^{-1}) and G418 (200 mg l^{-1}). Positive *cna1*Δ *hog1*Δ strains were screened by diagnostic PCR for the 5′ and 3′ junctions and further confirmed by Southern blot analysis (not shown).

To construct the serotype A *cna1*Δ + *CNA1* complemented strain, H99 genomic DNA containing the full-length *CNA1* gene was isolated from a *C. neoformans* H99 bacterial artificial chromosome (BAC) library by colony hybridization with a *CNA1* gene-specific probe amplified by PCR. The 5·7 kb *Bgl*II–*Bam*HI fragment containing the full-length *CNA1* gene was subcloned into pJAF12 (Neo^r), generating plasmid pNEOCNA1A. *Not*I-digested linearized pNEOCNA1A DNA was introduced by biolistic transformation into strain KK1 (Table 1) and integrated at the genomic *CNA1* locus. Integration of plasmid pNEOCNA1A was confirmed by Southern blotting.

Antifungal drug activity tests. For fludioxonil sensitivity testing on agar media, each strain was incubated overnight in liquid YPD medium at 30 °C and subcultured in fresh liquid YPD medium to OD_{600} 0·7–0·9. Then cells were serially diluted (10^1–10^5) in dH_2O, and spotted (2 μl) onto YPD agar containing 1 or 10 μg fludioxonil ml^{-1}, dissolved in DMSO.

The MICs of antifungal drugs for *C. neoformans* strains were assessed in accordance with the National Committee for Clinical Laboratory Standards (NCCLS) criteria for antifungal drug activity as previously described (Cruz *et al.*, 2002). Briefly, *In vitro* testing was performed in RPMI 1640 medium containing L-glutamine without sodium bicarbonate (Gibco), buffered to pH 7·0 with 0·165 M MOPS using 96-well plates (96-well cell culture cluster, flat-bottom; Costar). The fludioxonil concentrations tested were 10, 5, 1, 0·5, 0·1, 0·02, 0·01 and 0·005 μg ml^{-1}. Cells were incubated at 30 °C without shaking, and after 72 h, the OD_{600} was determined with a microtitre plate reader (Molecular Devices Thermomax). The MIC_{80} of fludioxonil was defined as the drug concentration at which 80 % reduction in optical density is observed compared with the no-drug control. Minimum fungicidal concentrations (MFCs) were determined by sampling 100 μl from each well that showed growth inhibition in the MIC assay and incubation on YPD medium at 30 °C for 72 h. The lowest concentration that yielded three or fewer colonies was recorded as the MFC.

The fractional inhibitory concentrations (FICs) and indexes were calculated as previously described (Cruz *et al.*, 2002). The FIC index is the sum of the FICs for each drug, which in turn is defined as the MIC_{80} of each drug when used in combination divided by the MIC_{80} of the drug when used alone. Based on the FIC index, drug interactions were classified as synergistic (FIC < 1·0), additive (FIC = 1·0), autonomous (FIC between 1 and 2) or antagonistic (FIC > 2). In the MFC and FIC experiments, FK506 was tested at 2, 0·5, 0·1 and 0·04 μg ml^{-1} as the final drug concentrations. For calculation purposes, MICs of < 5·0, > 2·0, ⩽ 0·5 and ⩽ 0·04 were assumed to be 5·0, 2·0, 0·5 and 0·04 respectively.

Western blot analysis of Hog1 phosphorylation. Yeast cells were grown to mid-exponential phase as described above, added to an equal volume of YPD medium containing 2 M NaCl, 2 μg or 20 μg fludioxonil ml^{-1} (final 1 M NaCl, 1 μg or 10 μg fludioxonil ml^{-1}), and further incubated for the indicated amount of time. Protein extraction and measurement of concentration were performed as described previously (Bahn *et al.*, 2005). An equal amount of protein (20 μg) was loaded into a 10 % Tris/glycine gel (Novex). Separated proteins were further transferred to Immunoblot PVDF membrane (Bio-Rad) and incubated at 4 °C overnight with a rabbit anti-dually phosphorylated p38 antibody (Cell Signalling) and for 1 h with a secondary anti-rabbit IgG horseradish-peroxidase-conjugated antibody. The blot was developed using the ECL Western Blotting Detection System (Amersham Bioscience). Subsequently, the blot was

stripped and further used for detection of Hog1 with a rabbit polyclonal anti-Hog1 antibody (Santa Cruz Biotechnology) as loading control.

Microscopy. Strains were inoculated into liquid YPD medium and grown overnight at 30 °C. The cells were washed with sterile dH_2O and reincubated in RPMI 1640 medium containing fludioxonil for 48 h. The cells were resuspended in dH_2O, and observed with a Zeiss Axioskop 2 equipped with an AxioCam MRM digital camera.

Intracellular glycerol measurement assay. To measure the intracellular glycerol content, each strain was grown to mid-exponential phase, added to an equal volume of YPD medium containing 20 μg fludioxonil ml^{-1} (final 10 μg fludioxonil ml^{-1}), and further incubated for the indicated amount of time. After incubation, cells were collected by centrifugation, washed with dH_2O and then extracted by boiling at 100 °C for 10 min. After centrifugation, the glycerol concentration in the supernatant was measured using a UV-glycerol assay kit according to the manufacturer's instructions (R-Biopharm). The same amount of each sample was lyophilized to measure cellular dry weight for normalization.

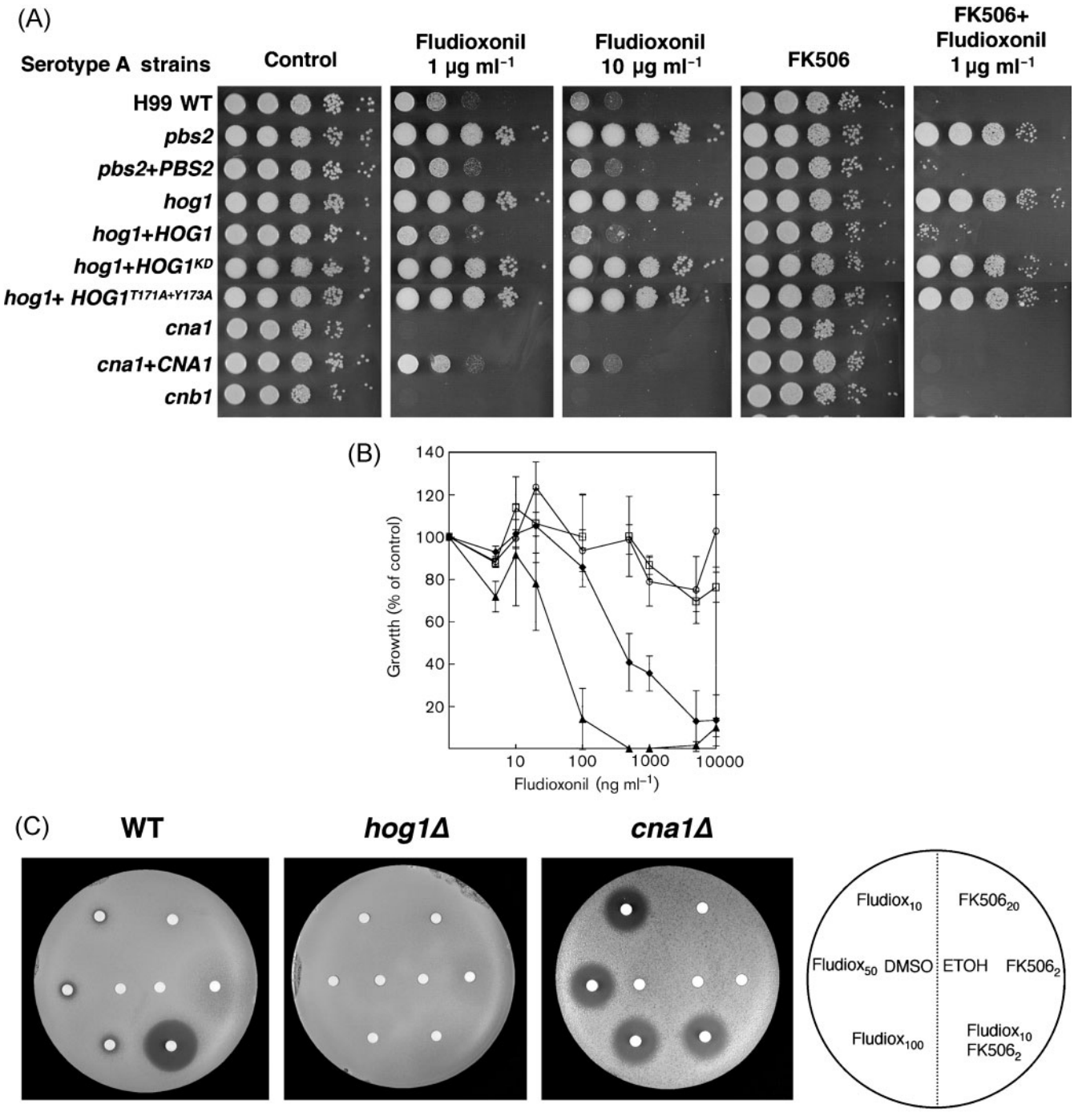

RESULTS

Multiple signalling pathways mediate the action of fludioxonil against *C. neoformans*

To investigate whether *C. neoformans* is sensitive to fludioxonil, fungal growth was tested on YPD agar containing the drug. Fludioxonil severely inhibited growth of the serotype A wild-type (WT) strain H99 in a dose dependent manner (Fig. 1A). To elucidate the role of the HOG pathway in fludioxonil sensitivity, we tested the sensitivity of *hog1*Δ and *pbs2*Δ mutants that had been constructed before (Bahn *et al.*, 2005). Both mutants exhibited complete resistance to fludioxonil, indicating that the Hog1 pathway is involved in fludioxonil sensitivity of *C. neoformans* (Fig. 1A). To examine whether phosphorylation and kinase activity of Hog1 MAPK are required to confer fludioxonil sensitivity, we tested the sensitivity of cells expressing site-directed mutants of Hog1 at the phosphorylation sites ($hog1+HOG1^{T171A+Y173A}$) or the catalytic site ($hog1+HOG1^{K49S+K50N}$) (Fig. 1A). These Hog1 mutants were as resistant to fludioxonil as the *hog1*Δ mutant, indicating that Pbs2-dependent phosphorylation and catalytic activation of the Hog1 MAPK are prerequisites for fludioxonil sensitivity (Fig. 1A).

A recent report revealed that cellular growth is reciprocally regulated by the calcineurin and HOG pathways in *S. cerevisiae* (Shitamukai *et al.*, 2004). Given the role of the HOG pathway in fludioxonil sensitivity of *C. neoformans*, we tested whether calcineurin is also involved in resistance to fludioxonil. For this purpose, we deleted the genes encoding the calcineurin catalytic (*CNA1*) or regulatory subunit (*CNB1*) in the H99 background with dominant selectable markers. The *cna1*Δ and *cnb1*Δ mutants exhibited hypersensitivity to fludioxonil, indicating that calcineurin promotes resistance to fludioxonil in *C. neoformans* (Fig. 1A). To further examine this hypothesis, we tested whether a synergistic fungicidal effect would be observed with concomitant exposure to fludioxonil and the calcineurin inhibitor FK506. In fact, FK506 greatly enhanced growth inhibition when combined with fludioxonil, but had no effect on cell growth by itself (Fig. 1A), strongly suggesting a synergistic fungicidal effect between the two drugs. Interestingly, a *cna1*Δ *hog1*Δ double mutant still exhibited complete resistance to fludioxonil (Fig. 1B), indicating that calcineurin-dependent fludioxonil resistance is also mediated directly or indirectly by the Hog1 MAPK.

To quantitatively measure fludioxonil sensitivity, we performed drug susceptibility assays according to NCCLS criteria using a range of fludioxonil concentrations (5 ng ml^{-1} to 10 μg ml^{-1}). In this assay, the MIC_{80} of fludioxonil for the WT strain was <5 μg ml^{-1} whereas the MIC_{80} for the *cna1*Δ mutant was <100 ng ml^{-1} (Fig. 1B, Table 2). In contrast, *hog1*Δ and *cna1*Δ *hog1*Δ mutants exhibited a modest reduction of growth, but still showed robust resistance, even with 10 μg fludioxonil ml^{-1} (Fig. 1B). Taken together, these findings indicate that sensitivity of *C. neoformans* to fludioxonil is oppositely regulated by the HOG and calcineurin pathways.

Fludioxonil in combination with FK506 exhibits fungicidal activity against *C. neoformans*

To demonstrate the synergism between fludioxonil and FK506 in *C. neoformans*, we employed disk diffusion halo assays. Even a disk containing 100 μg fludioxonil exerted only modest growth inhibition of the WT strain H99. Growth of the WT strain was not inhibited by FK506 under these conditions. However, when fludioxonil was combined with FK506, the halo produced was completely clear and larger than the haloes produced by fludioxonil alone (Fig. 1C). To confirm that calcineurin was the target of the observed drug synergy with FK506, a *cna1*Δ mutant strain was also tested. When disks containing 10, 50 or 100 μg fludioxonil were placed over the *cna1*Δ strain, we observed large haloes similar to those of the wild-type strain exposed to fludioxonil in combination with FK506 (Fig. 1C). Fludioxonil and FK506 did not produce any haloes on the *hog1*Δ strain, which is consistent with the result that the *hog1*Δ mutant was resistant to medium

Fig. 1. The Hog1 MAPK and calcineurin pathways regulate fludioxonil sensitivity in an opposing manner. (A) Each *C. neoformans* strain [WT (H99), *pbs2*Δ (YSB123), $pbs2\Delta+PBS2$ complemented (YSB212), *hog1*Δ (YSB64), $hog1\Delta+HOG1$ complemented (YSB145), $hog1\Delta+HOG1^{K49S+K50N}$ (YSB308), $hog1\Delta+HOG1^{T171A+Y173A}$ (YSB253), *cna1*Δ (KK1), $cna1\Delta+CNA1$ complemented (KK5), *cnb1*Δ (KK2), *cna1*Δ *hog1*Δ (KK4)] was grown to mid-exponential phase in liquid YPD medium, 10-fold serially diluted (10^1–10^5 dilutions), and spotted (2 μl dilution) on YPD agar containing 0, 1 or 10 μg fludioxonil ml^{-1}, 1 μg FK506 ml^{-1}, or both 1 μg FK506 ml^{-1} and 1 μg fludioxonil ml^{-1}. Cells were incubated at 30 °C for 48 h and photographed. (B) Cells were precultured in YPD medium at 30 °C for 16–20 h. After washing, approximately 2×10^3 cells were inoculated in 200 μl RPMI 1640 medium containing fludioxonil. The final fludioxonil concentrations tested were 10, 5, 1, 0·5, 0·1, 0·2, 0·01 and 0·005 μg ml^{-1}. After incubation at 30 °C for 72 h, cell density was determined as OD_{600}. Data represented are the mean ± SD from three independent experiments. The following serotype A strains were used for this assay: WT (H99) (◆), and *cna1*Δ (▲), *hog1*Δ (□) and *cna1*Δ *hog1*Δ (○) mutant strains. (C) WT (H99), *hog1*Δ and *cna1*Δ mutants were grown in YPD medium for 48 h. For each strain, 2×10^7 cells were resuspended in top agar and poured onto YPD agar medium. Disks containing combinations of 10 μg ($Fludiox_{10}$), 50 μg ($Fludiox_{50}$) or 100 μg ($Fludiox_{100}$) of fludioxonil, 2 μg ($FK506_2$) or 20 μg ($FK506_{20}$) of FK506, 5 μl of 100 % ethanol (ETOH) and dimethyl sulfoxide (DMSO), as indicated, were placed over the solidified top agar. Cells were incubated for 48 h at 30 °C.

Table 2. Combination of fludioxonil and FK506 exhibits synergistic effect on *C. neoformans*

Genotype (*C. neoformans* strain)	MIC_{80} alone (μg ml^{-1})		MIC_{80} combined (μg ml^{-1})* Fludiox/FK506	FIC index Fludiox/FK506
	Fludiox	FK506		
Wild-type (H99)	$<5{\cdot}0$	$>2{\cdot}0$	$\leqslant 0{\cdot}5/\leqslant 0{\cdot}04$	0·12
*cna1*Δ (KK1)	$<0{\cdot}1$	$>2{\cdot}0$	–	–
*hog1*Δ (YSB64)	$>10{\cdot}0$	$>2{\cdot}0$	–	–

*Combined MICs, expressed as [Fludioxonil]/[FK506], are the minimum concentrations of fludioxonil and FK506 that resulted in a fungicidal inhibition profiled when the two drugs were used in combination.

containing fludioxonil and FK506 (Fig. 1A, C). Additionally, the fractional inhibitory concentration (FIC) was calculated to determine the FIC index, of which a value $<1{\cdot}0$ denotes a synergistic interaction. The calculated FIC index of fludioxonil is 0·12 with FK506, denoting a synergistic relationship between fludioxonil and FK506 (Table 2). These results indicate that FK506 participates in drug synergy with fludioxonil by inhibiting the calcineurin pathway.

To determine whether fludioxonil is fungicidal or fungistatic to *C. neoformans*, minimal fungicidal concentrations (MFCs) were investigated in accordance with the NCCLS criteria (Table 3). Although fludioxonil dramatically inhibited growth of the WT strain in liquid medium (Fig. 1B), 10 μg fludioxonil ml^{-1} did not produce an MFC against the WT strain, indicating that fludioxonil at <10 μg ml^{-1} is not fungicidal against *C. neoformans* (Table 3). On the other hand, when fludioxonil was tested in combination with FK506, the MFC of fludioxonil was $\leqslant 0{\cdot}5$ μg ml^{-1}, indicating that the combination treatment of fludioxonil with FK506 has a fungicidal effect on the WT strain (Table 3). The MFC of fludioxonil for the *cna1*Δ mutant was $\leqslant 0{\cdot}5$ μg ml^{-1}, which is consistent with the MFC of fludioxonil in combination with FK506 against the WT strain.

Differential fungicidal sensitivity between serotypes

Our recent studies demonstrated that the HOG pathway is differentially regulated in the serotype A strain H99 and the serotype D strain JEC21 (Bahn *et al.*, 2005). Therefore, we hypothesized that fludioxonil sensitivity could also be differentially regulated between the two strains if it is controlled by the HOG pathway. In fact, the serotype D strain JEC21 exhibited complete resistance to fludioxonil, similar to the serotype A *hog1*Δ mutant; this is in stark contrast to the sensitivity of the WT serotype A strain H99 (Fig. 2). *S. cerevisiae* exhibits a similar Hog1 regulatory pattern to the JEC21 *C. neoformans* strain (Bahn *et al.*, 2005) and was also completely resistant to fludioxonil (Fig. 2).

Hog1 activation confers fludioxonil sensitivity in *C. neoformans*

It was recently reported that Hog1 is phosphorylated and activated in response to fludioxonil in several plant-pathogenic fungi, including *Colletotrichum lagenarium*, *Cochliobolus heterostrophus* and *Botrytis cinerea* (Kojima *et al.*, 2004). However, we have recently shown that Hog1 is constitutively phosphorylated under normal conditions and dephosphorylated in response to osmotic shock in the *C. neoformans* serotype A strain H99 (Bahn *et al.*, 2005). We therefore examined how Hog1 is regulated in response to fludioxonil in *C. neoformans*. For this purpose, Hog1 phosphorylation patterns were monitored in response to fludioxonil by Western blot analysis. When the serotype A strain H99 was exposed to 1 or 10 μg fludioxonil ml^{-1}, Hog1 was dephosphorylated within 15 min and its dephosphorylation status was maintained for 3 h (Fig. 3). This regulatory pattern is quite similar to that of Hog1 in the H99 strain under osmotic stress (Fig. 3), indicating that

Table 3. Fludioxonil is potently fungicidal in combination with the calcineurin inhibitor FK506

Genotype (*C. neoformans* strain)	MFC alone (μg ml^{-1})		MFC combined (μg ml^{-1})* Fludiox/FK506
	Fludiox	FK506	
Wild-type (H99)	$>10{\cdot}0$	$>2{\cdot}0$	$\leqslant 0{\cdot}5/\leqslant 0{\cdot}04$
*cna1*Δ (KK1)	$\leqslant 0{\cdot}5$	$>2{\cdot}0$	$\leqslant 0{\cdot}5/\leqslant 0{\cdot}0$
*hog1*Δ (YSB64)	$>10{\cdot}0$	$>2{\cdot}0$	$>10{\cdot}0/>2{\cdot}0$

*Combined MFCs, expressed as [Fludioxonil]/[FK506], are the minimum concentrations of fludioxonil and FK506 that resulted in a fungicidal inhibition profiled when the two drugs were used in combination.

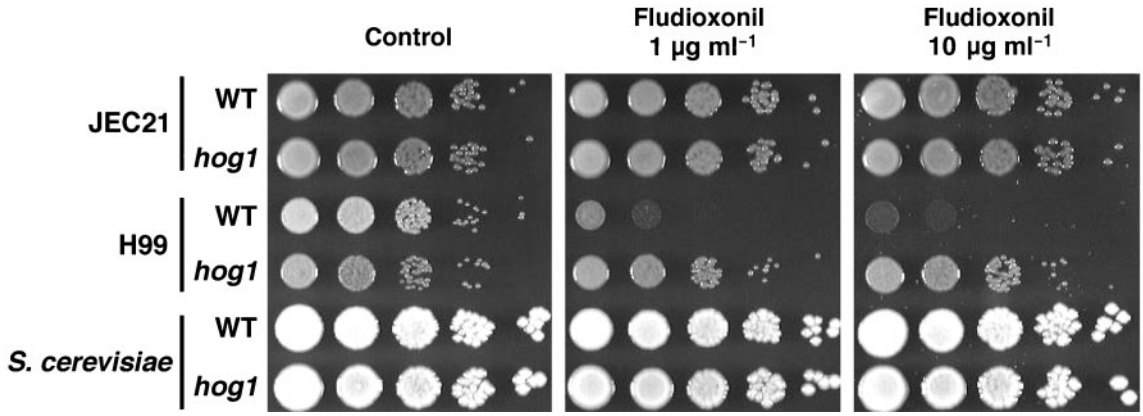

Fig. 2. Serotype D strain JEC21 and *S. cerevisiae* are resistant to fludioxonil. Fludioxonil sensitivity tests were performed as described in Fig. 1 with the following strains: serotype D WT strain JEC21 and *hog1*Δ (YSB139), serotype A WT strain H99 and *hog1*Δ (YSB64), *S. cerevisiae* diploid WT strain BY4743 and the homozygous *hog1*Δ/*hog1*Δ mutant.

fludioxonil activates the Hog1 pathway in WT H99 cells. On the other hand, in the serotype D strain JEC21 Hog1 was only slightly phosphorylated under normal conditions, only minimally further phosphorylated if at all after 15 min of exposure to fludioxonil, and subsequently maintained in an unphosphorylated state for up to 3 h (Fig. 3). In contrast, Hog1 was rapidly phosphorylated in response to osmotic shock in strain JEC21, as reported previously (Bahn *et al.*, 2005). Therefore, we conclude that Hog1 is rapidly activated by dephosphorylation in response to fludioxonil in the drug-sensitive H99 strain, whereas Hog1 is only minimally activated, if at all, in the presence of fludioxonil in the resistant serotype D strain JEC21. Hog1 was also found to be completely inactive during exposure to fludioxonil in *S. cerevisiae*, which is also resistant to fludioxonil (Fig. 3).

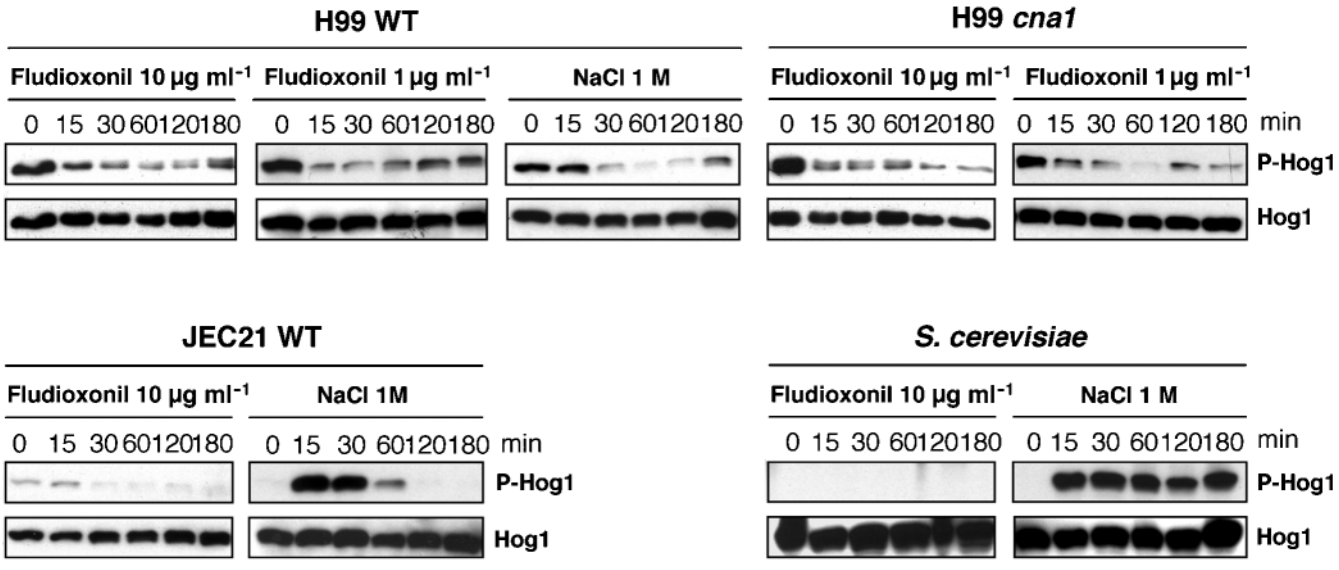

Fig. 3. The Hog1 MAPK in the serotype A strain H99 is activated by rapid dephosphorylation in response to fludioxonil. *C. neoformans* serotype A WT strain (H99) and *cna1*Δ (KK1), serotype D WT strain (JEC21), and *S. cerevisiae* diploid WT strain (BY4743) were grown to mid-exponential phase and treated with 1 or 10 μg fludioxonil ml^{-1} or 1 M NaCl in liquid YPD medium for the time indicated and total protein extracts were prepared for Western blot analysis. The dual phosphorylation status of Hog1 (T171 and Y173) was monitored using antibody specific for dual phosphorylation of p38 MAPK (P-Hog1). The same blot was stripped and then probed with polyclonal anti-Hog1 antibody as a loading control (Hog1).

We hypothesized that Hog1 might be hyperactivated in the calcineurin A *cna1*Δ mutant that is hypersensitive to fludioxonil (Fig. 1A–C). To address this, we monitored the Hog1 phosphorylation pattern of the *cna1*Δ mutant in response to fludioxonil. The Hog1 phosphorylation pattern in the *cna1*Δ mutant exposed to 1 μg or 10 μg fludioxonil ml^{-1} was almost identical to that observed in the wild-type strain in response to fludioxonil (Fig. 3). The data indicate that the calcineurin pathway promotes fludioxonil resistance, but does not directly regulate Hog1 phosphorylation or activation.

A question remains whether the differential fludioxonil sensitivity observed between the serotype A strain H99 and the serotype D strain JEC21 results from serotype- or strain-specific differences. Previously, we have shown that the H99-type Hog1 phosphorylation pattern predominates in a majority of *C. neoformans* strains regardless of serotype (Bahn *et al.*, 2005). Therefore, we investigated fludioxonil sensitivity in multiple serotype A and D clinical and environmental strains, and monitored the Hog1 phosphorylation pattern after a 1 h exposure to fludioxonil. A majority of *C. neoformans* strains (8 of 10 serotype A and 6 of 9 serotype D strains) were found to be sensitive to fludioxonil, and in these strains Hog1 was regulated in a manner similar to that of the H99 strain (Fig. 4A, B). Two serotype A strains (IN-38 and UG-20020), and three serotype D strains (NIH433, JEC21, MMRL757) exhibited clear resistance to fludioxonil (Fig. 4A, B). In the resistant strains, the Hog1 phosphorylation signal was almost undetectable under normal conditions, and this dephosphorylated state persisted after 1 h incubation with fludioxonil, indicating that Hog1 is not activated in response to fludioxonil. Taken together, these data demonstrate that fludioxonil exerts a fungicidal effect via activation of the Hog1 pathway in a majority of *C. neoformans* strains.

Fludioxonil sensitivity is a recessive phenotype

To investigate whether fludioxonil sensitivity is a dominant or recessive phenotype, we monitored the fludioxonil sensitivity of AD hybrid strains, which were laboratory-generated by crossing between strains JEC171 (*ade2 lys2*) and H99 (*ura5*) (Lengeler *et al.*, 2001). As expected, the parental control serotype A H99 (*ura5*) and serotype D JEC171 (*ade2 lys2*) strains exhibited sensitivity and resistance to fludioxonil, respectively (Fig. 5). All of 12 independently derived AD hybrid strains exhibited resistance similar to the parental strain JEC171, indicating that fludioxonil sensitivity is a recessive phenotype (Fig. 5 and data not shown).

Hog1 activation results in morphological defects

To investigate the cellular state in the presence of fludioxonil, we microscopically observed cells after exposure to fludioxonil. In the WT, some cells were swollen, and interestingly were often attached to each other, indicating a defect in cytokinesis during cell division (Fig. 6A-b). Although the *cna1*Δ mutant strain exhibited a cytokinesis defect without fludioxonil, when this mutant strain was treated with fludioxonil, the cells exhibited an even more severe cytokinesis defect (Fig. 6A-c). On the other hand, a majority of *hog1*Δ mutant cells exhibited no swollen morphology or defects in cell division (Fig. 6A-d). As expected, the morphology of JEC21 cells was not affected by fludioxonil (data not shown). These results demonstrate that fludioxonil-mediated cell growth inhibition is accompanied by defects in cell morphology and cell cycle that are dependent on integrity of the Hog1 pathway.

Hog1 activation by fludioxonil promotes glycerol accumulation

Next we addressed how fludioxonil treatment causes morphological defects. It has been previously reported that fludioxonil treatment stimulates glycerol accumulation in *N. crassa* (Fujimura *et al.*, 2000a). Therefore, we hypothesized that fludioxonil treatment hyperactivates the HOG pathway to stimulate excessive glycerol accumulation, which may cause morphological defects, including cell swelling. To test this hypothesis, we measured the glycerol content in *C. neoformans* after fludioxonil treatment for 1 and 3 h (Fig. 6B). In the WT strain H99, the glycerol content increased after 1 h exposure, and to an even greater extent after 3 h incubation. In contrast, no increase in glycerol was observed in the *hog1*Δ mutant compared to the WT. These results indicate that fludioxonil treatment hyperactivates the Hog1 osmotic response pathway, which results in overaccumulation of intracellular glycerol. Increased intracellular glycerol levels may trigger non-physiological levels of water influx into the cell, resulting in cell swelling and growth inhibition. In the *cna1*Δ mutant, intracellular glycerol content increased following 1 h treatment with fludioxonil but accumulation levels at 3 h were lower than those of the WT (Fig. 6B). Thus, the *cna1*Δ mutant does not maintain intracellular glycerol levels similar to the WT strain, and may release glycerol to the extracellular environment, possibly due to impaired cell wall integrity. Alternatively, the *cna1*Δ mutant cells could be rapidly killed by Hog1 activation prior to accumulating glycerol, because fludioxonil has a fungicidal effect on the *cna1*Δ mutant (Table 2). As expected, the resistant strain JEC21 accumulated little or no glycerol after treatment with fludioxonil compared to the H99 WT or *cna1*Δ mutant strains (Fig. 6B), further supporting our finding that Hog1 is not activated in strain JEC21 in response to fludioxonil (Fig. 3).

Cell wall integrity is required for resistance to fludioxonil

To test whether general defects in cell wall integrity result in hypersensitivity to fludioxonil, we examined the fludioxonil sensitivity of a mutant lacking the *MPK1* MAPK gene, which is also known to regulate cell wall integrity in *C. neoformans* (Kraus *et al.*, 2003) In accord with this hypothesis, the *mpk1*Δ mutant exhibited a growth defect at 37 °C (data not

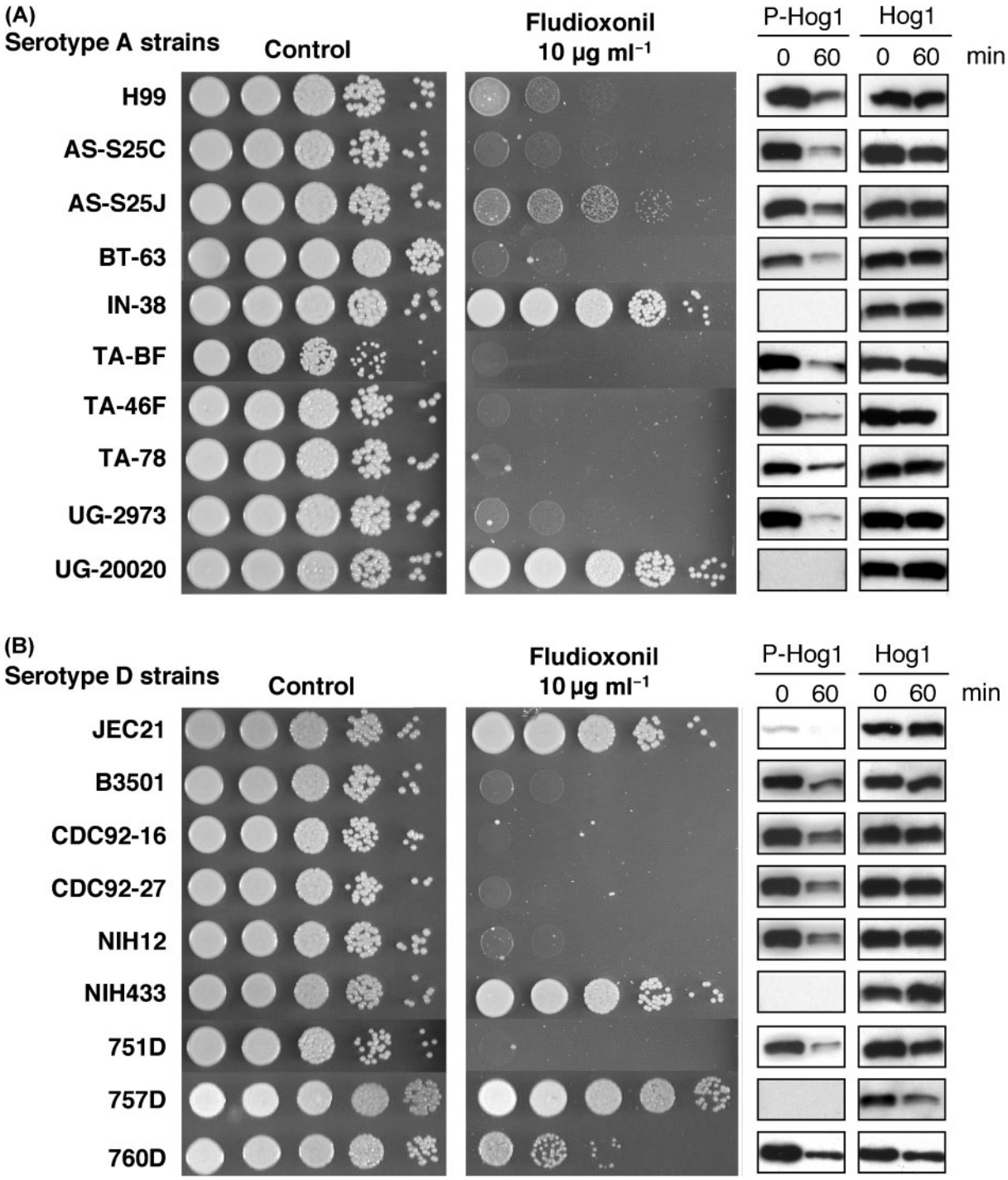

Fig. 4. A majority of serotype A and D strains exhibit fludioxonil sensitivity in a Hog1-dependent manner. Fludioxonil sensitivity and Hog1 phosphorylation patterns were monitored in various clinical and environmental serotype A (A) and D (B) isolates. Drug sensitivity tests and Western blot were performed as described in Figs 1 and 3 respectively. For serotype A, nine clinical strains isolated from Asia [S25C (second row) and S25J (third row)], Botswana [BT-63 (fourth row)], India [IN-38 (fifth row)], Tanzania [BF (sixth row), 46F.5.02 (seventh row) and 78.7.98 (eighth row)] and Uganda [2973 (ninth row) and 20020 (tenth row)] were used. For serotype D, CDC92-16, CDC92-27, MMRL751, MMRL757 and MMRL760 (listed as 751D, 757D and 760D in the figure) were monitored as clinical strains. NIH12 and NIH433 are the parental clinical and environmental strains, respectively, for B3501 and JEC21 (Heitman *et al.*, 1999).

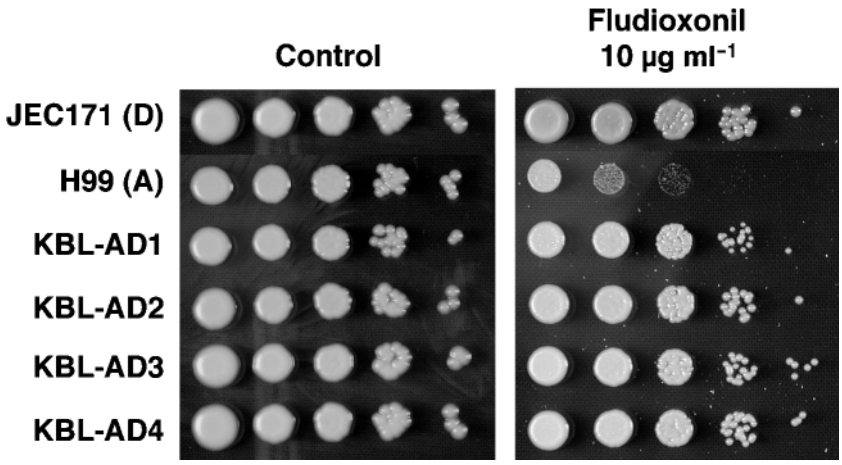

Fig. 5. Fludioxonil sensitivity is a recessive phenotype. Fludioxonil sensitivity was assayed as described in Fig. 1 with the following strains: serotype D strain JEC171, serotype A strain H99 (5-FOA resistant) and AD hybrid strains KBL-AD1, KBL-AD2, KBL-AD3 and KBL-AD4 (Lengeler *et al.*, 2001).

shown) and hypersensitivity to fludioxonil similar to that of the *cna1*Δ mutant (Fig. 7). In addition, *C. neoformans* mutants lacking the highly conserved *MKK1* and *BCK1* genes, which encode a MAPK kinase (MAPKK) and a MAPKK kinase (MAPKKK), respectively, which function upstream of the Mpk1 MAPK, also showed hypersensitivity to fludioxonil (Fig. 7). Interestingly, supplementation with 1 M sorbitol as an osmotic stabilizer partially rescued the growth defect of the *mpk1*Δ, *mkk1*Δ and *bck1*Δ mutants in response to fludioxonil treatment. These results further support models in which cell wall integrity promotes cell viability in the presence of fludioxonil.

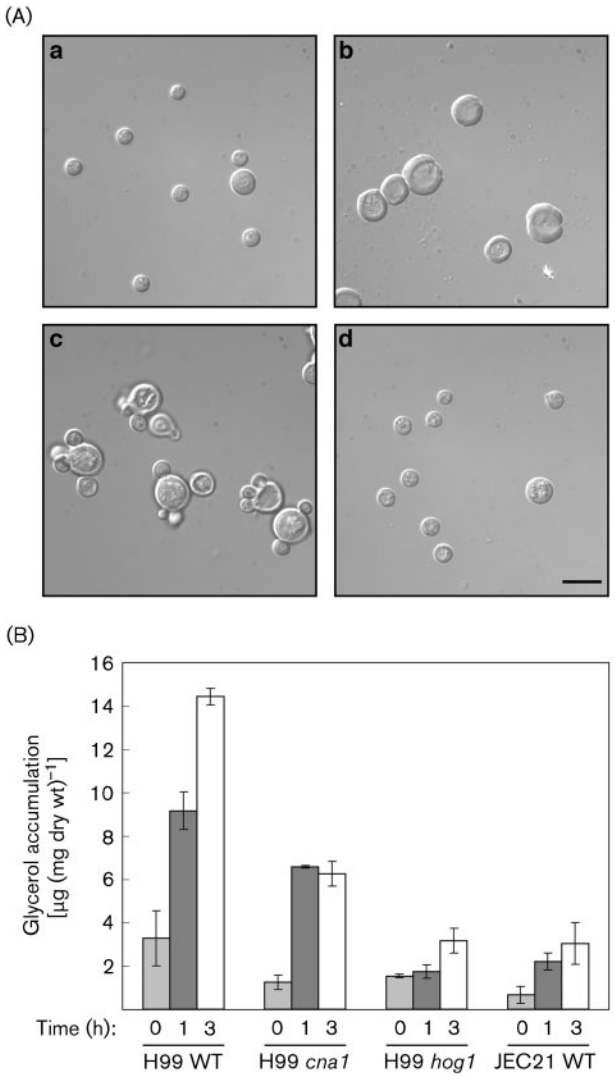

Fig. 6. Fludioxonil treatment causes morphological changes in drug-sensitive strains. (A) Serotype A WT strain (H99; a, b), the *cna1*Δ mutant (KK1; c), and the *hog1*Δ mutant (YSB64; d) were grown to mid-exponential phase in liquid YPD. Cells were reincubated in RPMI 1640 medium containing 10 μg fludioxonil ml^{-1} for 48 h without shaking. As a control, WT cells were incubated in RPMI 1640 medium without fludioxonil (a). Cells were observed by microscopy. Bar, 20 μm. (B) Fludioxonil-sensitive strains exhibit glycerol accumulation in a Hog1-dependent manner. To measure glycerol content, serotype A WT strain H99, *cna1*Δ (KK1) and *hog1*Δ (YSB64) mutant strains, and the serotype D WT strain JEC21, were grown to mid-exponential phase and then incubated in liquid YPD medium with 10 μg fludioxonil ml^{-1} for the time indicated. Glycerol content in cell extracts was measured by a UV-glycerol assay procedure as described in Methods and normalized to dry cell weight. Two individual experiments were performed. Standard deviations are presented as error bars.

DISCUSSION

In this study, we demonstrated that the phenylpyrrole drug fludioxonil exerts an antifungal activity against the basidiomycetous human fungal pathogen *C. neoformans*. In fungi that infect plants, it has been shown that the fungicidal activity of fludioxonil is mediated through activation of the Hog1 MAPK pathway (Kojima *et al.*, 2004). Here, we propose a model in which *C. neoformans* sensitivity to fludioxonil is not only positively controlled by the HOG pathway, but also negatively controlled by the calcineurin and Mpk1 MAPK pathways, which are involved in maintaining cell wall integrity (Fig. 8). In this model, the Hog1

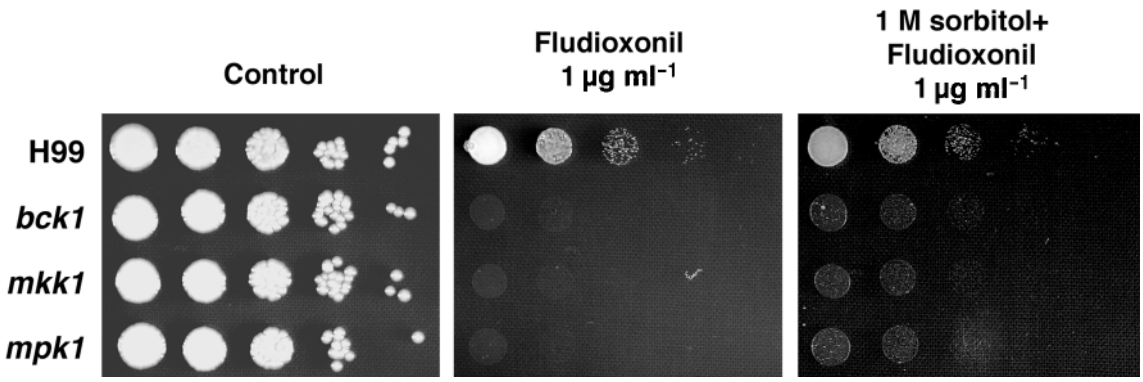

Fig. 7. Cell wall integrity defects cause hypersensitivity to fludioxonil. *C. neoformans* serotype A WT (H99), and *mpk1*Δ (KK3), *mkk1*Δ (YSB330) and *bck1*Δ (YSB273) mutant strains, were inoculated on YPD agar containing 1 µg fludioxonil ml^{-1} with or without 1 M sorbitol, and incubated at 30 °C for 48 h.

MAPK in a majority of serotype A and D *C. neoformans* strains is activated by dephosphorylation in response to fludioxonil treatment, which in turn causes a rapid accumulation of intracellular glycerol, cell swelling, cytokinesis defects and cell growth inhibition. Several lines of evidence show that the Hog1 MAPK pathway plays a central role in promoting fludioxonil sensitivity in *C. neoformans*. First, *hog1*Δ and *pbs2*Δ mutants exhibited strong resistance to fludioxonil. Second, strain-specific variation in fludioxonil sensitivity in different *C. neoformans* strains is completely correlated with their Hog1 MAPK phosphorylation patterns. Independently, the calcineurin and the Mpk1 MAPK pathways promote resistance to fludioxonil via the cell wall integrity pathway (Fig. 8).

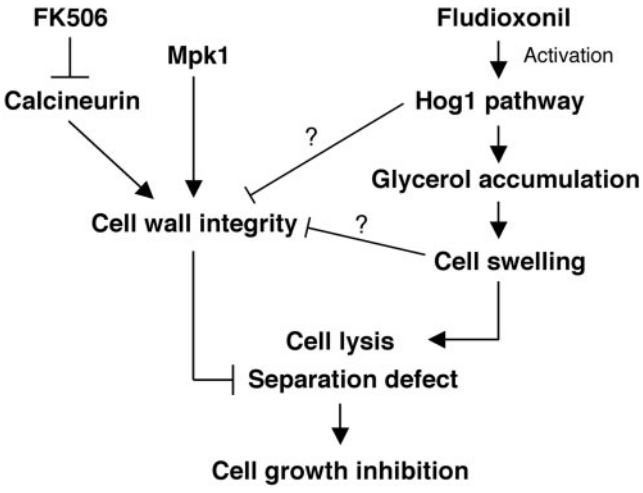

Fig. 8. Schematic diagram of pathways mediating antifungal effects on *C. neoformans*. Fludioxonil treatment activates the HOG pathway by rapid dephosphorylation of the Hog1 MAPK in the majority of *C. neoformans* strains, in which Hog1 is phosphorylated under normal conditions. Hog1 activation contributes to intracellular glycerol accumulation, causing cell swelling by rapid water influx and perturbing cell surface integrity, which may result in cell lysis or cytokinesis defects. On the other hand, the calcineurin and Mpk1 MAPK pathways independently contribute to fludioxonil resistance by promoting cell wall integrity.

Antifungal effects caused by fludioxonil treatment appear to be due to excessive accumulation of intracellular glycerol activated by the HOG pathway. In the budding yeast, the HOG pathway regulates various stress-response genes for osmoprotection, including *GPD1*, which encodes glycerol-3-phosphate dehydrogenase, an enzyme involved in glycerol synthesis (Albertyn *et al.*, 1994). However, we speculate that glycerol accumulation is not the only factor contributing to fungal toxicity exerted by fludioxonil. In *N. crassa*, a *cut* mutant, which was deficient in glycerol synthesis, remained sensitive to fludioxonil (Fujimura *et al.*, 2000b). We found that some WT cells, but not *hog1*Δ mutant cells, of *C. neoformans*, were attached to each other following fludioxonil exposure, indicating that normal cytokinesis is also affected by fludioxonil treatment via the Hog1 pathway. This cell–cell attachment was not attributable to cell aggregation after cell division because even sonication could not separate these avidly attached cells (data not shown).

Another novel finding in this study is that the cell wall integrity pathways, including the calcineurin and Mpk1 MAPK pathways, promote resistance to fludioxonil treatment. These pathways appear to contribute to fludioxonil resistance independent of Hog1 MAPK regulation because the *cna1*Δ mutation did not significantly change Hog1 phosphorylation patterns. In the model yeast *S. cerevisiae*, however, perturbation of the HOG pathway partially suppresses cell wall integrity defects via the SVG (STE vegetative growth) pathway that works in parallel with the Mpk1 pathway (Lee & Elion, 1999). In this process, the HOG pathway seems to negatively regulate cell wall integrity through the SVG pathway, antagonizing the Mpk1 MAPK pathway. Therefore, it is possible that overactivation of the

HOG1 pathway by fludioxonil treatment impairs cell wall integrity in *C. neoformans*, resulting in a cytokinesis defect (Fig. 8). Furthermore, fludioxonil hypersensitivity of the *mpk1*Δ mutant was partially suppressed by osmostabilization or incubation at low temperature (Fig. 7 and data not shown), suggesting that fludioxonil affects cell wall integrity in fungi. On the other hand, we speculate that fludioxonil treatment increases internal glycerol accumulation by Hog1 activation, which generates osmotic pressure to decrease cell wall integrity, which can be further affected by defects in the calcineurin or Mpk1 pathway (Fig. 8). Furthermore, decreased cell-wall integrity by fludioxonil might be involved in the cytokinesis defects. In *S. cerevisiae*, cytokinesis defects are observed in mutants deleted for genes encoding PIR (protein with internal repeat) family members, which are covalently attached to 1,3-β-glucan in the cell wall (Mrsa *et al.*, 1997; Mrsa & Tanner, 1999). These mutants also exhibit decreased cell wall integrity and a defect in mother–daughter cell separation (Teparic *et al.*, 2004).

The data from this study lead us to propose a unique way of treating cryptococcosis by simultaneously controlling two independent signalling pathways, the Hog1 MAPK and calcineurin pathways. Potential application of a combination drug therapy for treatment of human fungal pathogens has been proposed by others. The immunophilin-targeting drugs, FK506 and cyclosporin A, which are inhibitors of calcineurin, exhibit antifungal activity against several human fungal pathogens, such as *Candida albicans*, *Cryptococcus neoformans* and *Aspergillus fumigatus* (Cruz *et al.*, 2001; High, 1994; Odom *et al.*, 1997a). Combinations of a calcineurin inhibitor with an inhibitor of 1,3-β-glucan synthase or an inhibitor of ergosterol exhibit dramatic synergistic antifungal activity against these pathogens *in vitro* (Cruz *et al.*, 2002; Del Poeta *et al.*, 2000; Onyewu *et al.*, 2003; Steinbach *et al.*, 2004). In this study, we discovered a novel drug combination of fludioxonil and a calcineurin inhibitor that exhibited synergistic fungicidal activity against *C. neoformans*, in contrast to the fungistatic activity by fludioxonil alone. In plant-pathogenic fungi such as *Magnaporthe grisea* and *Botrytis cinerea*, a calcineurin inhibitor prevents development of infection-specific structures (Viaud *et al.*, 2003, 2002) and fludioxonil inhibits the growth of these fungi (Gehmann *et al.*, 1990), suggesting the possibility of a synergistic lethal impact on plant-pathogenic fungi by combining these drugs for agricultural use.

The protein target of fludioxonil remains to be elucidated. Notably, *C. neoformans* seems to contain an evolutionarily conserved phosphorelay system upstream of the Pbs2-Hog1 MAPK pathway. In contrast to *S. cerevisiae*, which contains only a single sensor kinase (Sln1), *C. neoformans* has seven putative two-component histidine-kinase-like proteins. The functions of these sensor proteins have not as yet been studied. Heterologous expression of *M. grisea* Hik1, a member of the Os-1 family of the two-component histidine kinases, can confer fludioxonil sensitivity to *S. cerevisiae* (Motoyama *et al.*, 2005). These observations indicate that Hik1 could be a direct fludioxonil target or a signalling mediator for its fungicidal action that activates the Hog1 pathway. In *N. crassa*, however, an intracellular cAMP and calcium-independent protein kinase binds fenpicolonil, which is a related phenylpyrrole fungicide (Pillonel & Mayer, 1997), raising the possibility that the phenylpyrrole class of drug could directly bind to targets in pathways other than the HOG pathway. Further characterization of upstream factors in the *C. neoformans* Hog1 MAPK, and of other signalling pathways that are related to fludioxonil sensitivity, may lead to the identification of the direct target of fludioxonil. At this point, we cannot exclude the possibility that signalling cross-talk may exist between the Hog1 pathway and other signalling pathways, and may play an important role in sensing and mediating antifungal action in *C. neoformans*. Furthermore, our data demonstrate that fludioxonil sensitivity is a recessive phenotype although the majority of *C. neoformans* strains are drug-sensitive. We speculate that during evolution *C. neoformans* might have lost either precise upstream regulation or downstream feedback control of Hog1, resulting in constitutive phosphorylation of the MAPK and contributing to fludioxonil sensitivity. Such evolutionary events may have provided selective benefits to the pathogen for host infection, such as high stress resistance. In conclusion, our study proposes new target pathways for the development of therapies for human fungal infections and expands options for the utility of existing antifungal drug classes, such as calcineurin inhibitors, by combination therapy with fludioxonil to exert synergistic antifungal effects.

ACKNOWLEDGEMENTS

We thank Jenny Lodge for signature-tagged markers and Chiatogu Onyewu, Deborah Fox and Jill Blankenship for advice and critically reading the manuscript. FK506 was generously provided by Fujisawa. This work was supported in part by NIH/NIAID R01 grants AI41937 and AI42159. Joseph Heitman was a Burroughs Wellcome Scholar in Molecular Pathogenic Mycology and an Investigator of the Howard Hughes Medical Institute.

REFERENCES

Albertyn, J., Hohmann, S., Thevelein, J. M. & Prior, B. A. (1994). *GPD1*, which encodes glycerol-3-phosphate dehydrogenase, is essential for growth under osmotic stress in *Saccharomyces cerevisiae*, and its expression is regulated by the high-osmolarity glycerol response pathway. *Mol Cell Biol* **14**, 4135–4144.

Bahn, Y. S., Kojima, K., Cox, G. M. & Heitman, J. (2005). Specialization of the HOG pathway and its impact on differentiation and virulence of *Cryptococcus neoformans*. *Mol Biol Cell* **16**, 2285–2300.

Borel, J. F. (1976). Comparative study of in vitro and in vivo drug effects on cell-mediated cytotoxicity. *Immunology* **31**, 631–641.

Cameron, M. L., Schell, W. A., Bruch, S., Bartlett, J. A., Waskin, H. A. & Perfect, J. R. (1993). Correlation of in vitro fluconazole resistance of *Candida* isolates in relation to therapy and symptoms of individuals seropositive for human immunodeficiency virus type 1. *Antimicrob Agents Chemother* **37**, 2449–2453.

Cruz, M. C., Del Poeta, M., Wang, P. & 7 other authors (2000). Immunosuppressive and nonimmunosuppressive cyclosporine analogs are toxic to the opportunistic fungal pathogen *Cryptococcus neoformans* via cyclophilin-dependent inhibition of calcineurin. *Antimicrob Agents Chemother* **44**, 143–149.

Cruz, M. C., Fox, D. S. & Heitman, J. (2001). Calcineurin is required for hyphal elongation during mating and haploid fruiting in *Cryptococcus neoformans*. *EMBO J* **20**, 1020–1032.

Cruz, M. C., Goldstein, A. L., Blankenship, J. R., Del Poeta, M., Davis, D., Cardenas, M. E., Perfect, J. R., McCusker, J. H. & Heitman, J. (2002). Calcineurin is essential for survival during membrane stress in *Candida albicans*. *EMBO J* **21**, 546–559.

Davidson, R. C., Blankenship, J. R., Kraus, P. R., de Jesus Berrios, M., Hull, C. M., D'Souza, C., Wang, P. & Heitman, J. (2002). A PCR-based strategy to generate integrative targeting alleles with large regions of homology. *Microbiology* **148**, 2607–2615.

Del Poeta, M., Cruz, M. C., Cardenas, M. E., Perfect, J. R. & Heitman, J. (2000). Synergistic antifungal activities of bafilomycin A(1), fluconazole, and the pneumocandin MK-0991/caspofungin acetate (L-743,873) with calcineurin inhibitors FK506 and L-685,818 against *Cryptococcus neoformans*. *Antimicrob Agents Chemother* **44**, 739–746.

Fox, D. S., Cruz, M. C., Sia, R. A., Ke, H., Cox, G. M., Cardenas, M. E. & Heitman, J. (2001). Calcineurin regulatory subunit is essential for virulence and mediates interactions with FKBP12-FK506 in *Cryptococcus neoformans*. *Mol Microbiol* **39**, 835–849.

Fraser, J. A., Subaran, R. L., Nichols, C. B. & Heitman, J. (2003). Recapitulation of the sexual cycle of the primary fungal pathogen *Cryptococcus neoformans* var. *gattii*: implications for an outbreak on Vancouver Island, Canada. *Eukaryot Cell* **2**, 1036–1045.

Fujimura, M., Ochiai, N., Ichiishi, A., Usami, R., Horikoshi, K. & Yamaguchi, I. (2000a). Fungicide resistance and osmotic stress sensitivity in *os* mutants of *Neurospora crassa*. *Pestic Biochem Physiol* **67**, 125–133.

Fujimura, M., Ochiai, N., Ichiishi, A., Usami, R., Horikoshi, K. & Yamaguchi, I. (2000b). Sensitivity to phenylpyrrole fungicides and abnormal glycerol accumulation in *os* and *cut* mutant strains of *Neurospora crassa*. *J Pestic Sci* **25**, 31–36.

Gehmann, K., Nyfeler, R., Leadbeater, A. J., Nevill, D. & Sozzi, D. (1990). CGA 173506: a new phenylpyrrole fungicide for broad-spectrum disease control. *Brighton Crop Prot Conf Pests Dis* **2**, 399–406.

Giaever, G., Chu, A. M., Ni, L. & 71 other authors (2002). Functional profiling of the *Saccharomyces cerevisiae* genome. *Nature* **418**, 387–391.

Heitman, J., Allen, B., Alspaugh, J. A. & Kwon-Chung, K. J. (1999). On the origins of congenic MATα and MAT**a** strains of the pathogenic yeast *Cryptococcus neoformans*. *Fungal Genet Biol* **28**, 1–5.

Hensel, M., Shea, J. E., Gleeson, C., Jones, M. D., Dalton, E. & Holden, D. W. (1995). Simultaneous identification of bacterial virulence genes by negative selection. *Science* **269**, 400–403.

High, K. P. (1994). The antimicrobial activities of cyclosporine, FK506, and rapamycin. *Transplantation* **57**, 1689–1700.

Hull, C. M. & Heitman, J. (2002). Genetics of *Cryptococcus neoformans*. *Annu Rev Genet* **36**, 557–615.

Kino, T., Hatanaka, H., Hashimoto, M., Nishiyama, M., Goto, T., Okuhara, M., Kohsaka, M., Aoki, H. & Imanaka, H. (1987). FK-506, a novel immunosuppressant isolated from a *Streptomyces*. I. Fermentation, isolation, and physico-chemical and biological characteristics. *J Antibiot* **40**, 1249–1255.

Kojima, K., Takano, Y., Yoshimi, A., Tanaka, C., Kikuchi, T. & Okuno, T. (2004). Fungicide activity through activation of a fungal signalling pathway. *Mol Microbiol* **53**, 1785–1796.

Kraus, P. R., Fox, D. S., Cox, G. M. & Heitman, J. (2003). The *Cryptococcus neoformans* MAP kinase Mpk1 regulates cell integrity in response to antifungal drugs and loss of calcineurin function. *Mol Microbiol* **48**, 1377–1387.

Kwon-Chung, K. J., Edman, J. C. & Wickes, B. L. (1992). Genetic association of mating types and virulence in *Cryptococcus neoformans*. *Infect Immun* **60**, 602–605.

Lee, B. N. & Elion, E. A. (1999). The MAPKKK Ste11 regulates vegetative growth through a kinase cascade of shared signaling components. *Proc Natl Acad Sci U S A* **96**, 12679–12684.

Lengeler, K. B., Cox, G. M. & Heitman, J. (2001). Serotype AD strains of *Cryptococcus neoformans* are diploid or aneuploid and are heterozygous at the mating-type locus. *Infect Immun* **69**, 115–122.

Moore, T. D. & Edman, J. C. (1993). The alpha-mating type locus of *Cryptococcus neoformans* contains a peptide pheromone gene. *Mol Cell Biol* **13**, 1962–1970.

Motoyama, T., Ohira, T., Kadokura, K., Ichiishi, A., Fujimura, M., Yamaguchi, I. & Kudo, T. (2005). An Os-1 family histidine kinase from a filamentous fungus confers fungicide-sensitivity to yeast. *Curr Genet* **47**, 298–306.

Mrsa, V. & Tanner, W. (1999). Role of NaOH-extractable cell wall proteins Ccw5p, Ccw6p, Ccw7p and Ccw8p (members of the Pir protein family) in stability of the *Saccharomyces cerevisiae* cell wall. *Yeast* **15**, 813–820.

Mrsa, V., Seidl, T., Gentzsch, M. & Tanner, W. (1997). Specific labelling of cell wall proteins by biotinylation. Identification of four covalently linked *O*-mannosylated proteins of *Saccharomyces cerevisiae*. *Yeast* **13**, 1145–1154.

Ochiai, N., Fujimura, M., Oshima, M., Motoyama, T., Ichiishi, A., Yamada-Okabe, H. & Yamaguchi, I. (2002). Effects of iprodione and fludioxonil on glycerol synthesis and hyphal development in *Candida albicans*. *Biosci Biotechnol Biochem* **66**, 2209–2215.

Odom, A., Del Poeta, M., Perfect, J. & Heitman, J. (1997a). The immunosuppressant FK506 and its nonimmunosuppressive analog L-685,818 are toxic to *Cryptococcus neoformans* by inhibition of a common target protein. *Antimicrob Agents Chemother* **41**, 156–161.

Odom, A., Muir, S., Lim, E., Toffaletti, D. L., Perfect, J. & Heitman, J. (1997b). Calcineurin is required for virulence of *Cryptococcus neoformans*. *EMBO J* **16**, 2576–2589.

Onyewu, C., Blankenship, J. R., Del Poeta, M. & Heitman, J. (2003). Ergosterol biosynthesis inhibitors become fungicidal when combined with calcineurin inhibitors against *Candida albicans*, *Candida glabrata*, and *Candida krusei*. *Antimicrob Agents Chemother* **47**, 956–964.

Orth, A. B., Rzhetskaya, M., Pell, E. J. & Tien, M. (1995). A serine (threonine) protein kinase confers fungicide resistance in the phytopathogenic fungus *Ustilago maydis*. *Appl Environ Microbiol* **61**, 2341–2345.

Paugam, A., Dupouy-Camet, J., Blanche, P., Gangneux, J. P., Tourte-Schaefer, C. & Sicard, D. (1994). Increased fluconazole resistance of *Cryptococcus neoformans* isolated from a patient with AIDS and recurrent meningitis. *Clin Infect Dis* **19**, 975–976.

Perfect, J. R. & Durack, D. T. (1985). Effects of cyclosporine in experimental cryptococcal meningitis. *Infect Immun* **50**, 22–26.

Perfect, J. R., Ketabchi, N., Cox, G. M., Ingram, C. W. & Beiser, C. L. (1993). Karyotyping of *Cryptococcus neoformans* as an epidemiological tool. *J Clin Microbiol* **12**, 3305–3309.

Pillonel, C. & Mayer, T. (1997). Effect of phenylpyrroles on glycerol accumulation and protein kinase activity of *Neurospora crassa*. *Pestic Sci* **49**, 229–236.

Ramesh, M. A., Laidlaw, R. D., Durrenberger, F., Orth, A. B. & Kronstad, J. W. (2001). The cAMP signal transduction pathway mediates resistance to dicarboximide and aromatic hydrocarbon fungicides in *Ustilago maydis*. *Fungal Genet Biol* **32**, 183–193.

Shitamukai, A., Hirata, D., Sonobe, S. & Miyakawa, T. (2004). Evidence for antagonistic regulation of cell growth by the calcineurin and high osmolarity glycerol pathways in *Saccharomyces cerevisiae*. *J Biol Chem* **279**, 3651–3661.

Steinbach, W. J., Schell, W. A., Blankenship, J. R., Onyewu, C., Heitman, J. & Perfect, J. R. (2004). In vitro interactions between antifungals and immunosuppressants against *Aspergillus fumigatus*. *Antimicrob Agents Chemother* **48**, 1664–1669.

Teparic, R., Stuparevic, I. & Mrsa, V. (2004). Increased mortality of *Saccharomyces cerevisiae* cell wall protein mutants. *Microbiology* **150**, 3145–3150.

Viaud, M. C., Balhadere, P. V. & Talbot, N. J. (2002). A *Magnaporthe grisea* cyclophilin acts as a virulence determinant during plant infection. *Plant Cell* **14**, 917–930.

Viaud, M., Brunet-Simon, A., Brygoo, Y., Pradier, J. M. & Levis, C. (2003). Cyclophilin A and calcineurin functions investigated by gene inactivation, cyclosporin A inhibition and cDNA arrays approaches in the phytopathogenic fungus *Botrytis cinerea*. *Mol Microbiol* **50**, 1451–1465.

White, T. C., Marr, K. A. & Bowden, R. A. (1998). Clinical, cellular, and molecular factors that contribute to antifungal drug resistance. *Clin Microbiol Rev* **11**, 382–402.

Zhang, Y., Lamm, R., Pillonel, C., Lam, S. & Xu, J. R. (2002). Osmoregulation and fungicide resistance: the *Neurospora crassa os-2* gene encodes a HOG1 mitogen-activated protein kinase homologue. *Appl Environ Microbiol* **68**, 532–538.